Demethylation. A more favorable dissociation energy of −126.8 kcal/mol, reaction 2, is obtained by fragmenting CH_6^{2+} into H_3^+ and CH_3^+. For this process, however, three "C–H bonds" have to be broken. Intuitively this suggests that an even higher barrier might be involved despite the larger exothermicity. After extensively searching at the 3-21G level we were able to locate this transition structure with C_s symmetry.[37] Our final estimate of the dissociation barrier is 59.9 kcal/mol (MP3/6-31G**//6-31G* + scaled ZPE).

Similarly we assume a significant barrier for the fragmentation of CH_6^{2+} into $H_2^{+}\cdot$ and $CH_4^{+}\cdot$ since two C–H bonds have to be cleaved in this near isothermic reaction 2. However, we did not investigate this process in detail.

Prospects for the Experimental Realization of CH_6^{2+}. Our work indicates that CH_6^{2+} should be a metastable dication with quite high dissociation barriers. How can CH_6^{2+} be generated? The reverse of reaction 4, the hydrogenation of CH_4^{2+}, may, because of the favorable thermodynamics (ΔE = 79.4 kcal/mol), be viewed as a possible mode for formation of CH_6^{2+}. Since CH_4^{2+} is reported to have a lifetime greater than 3 μs, and is generated by the mass-spectroscopic charge-transfer stripping technique from methane by a neutral collision gas (N_2),[8] mixing in of hydrogen might provide the conditions for the formation of CH_6^{2+}. Although electron transfer from H_2 to CH_4^{2+} (eq 5) and proton transfer

$$CH_4^{2+} + H_2 \rightarrow CH_4^{+}\cdot + H_2^{+}\cdot \qquad \Delta E = -102 \text{ kcal/mol} \quad (5)$$

$$CH_4^{2+} + H_2 \rightarrow CH_3^{+} + H_3^{+} \qquad \Delta E = -206 \text{ kcal/mol} \quad (6)$$

from CH_4^{2+} to H_2 (eq 6) are even more favorable, they are likely to have CH_6^{2+} as the intermediate species. We encourage mass spectrometrists to seek this dication.

Conclusions

The prototype of hexacoordinate carbon, CH_6^{2+}, is a minimum on the potential energy surface. Its C_{2v} geometry (**1**) has two stabilizing 3c-2e interactions. Despite the favorable thermodynamics for dissociation CH_6^{2+} appears to have sizable barriers for deprotonation and for loss of H_3^+. Within these barriers two polytopal rearrangements were established, rendering CH_6^{2+} subject to very fast H scrambling. Hydrogenation of CH_4^{2+}, by means of mass-spectroscopic charge stripping of CH_4 with inert gas and hydrogen, is suggested as a possible experimental approach to CH_6^{2+}.

Acknowledgment. The cooperation of the USC computer center greatly facilitated the present investigation. M.B. thanks the Consiglio Nazionale delle Ricerche (CNR) for the award of a National Scholarship for research abroad. The project benefited from senior scientist awards of the von Humboldt Foundation (to G.A.O. and J.A.P.) and support from the Fonds der Chemischen Industrie. We thank W. J. Hehre and G. A. Segal for constructive discussions and T. Clark, A. Sawaryn, and G. W. Spitznagel for some computations.

Registry No. CH_6^{2+}, 83561-00-6.

(37) The following procedure proved successful: in a first approach at the 3-21G level H_3^+ was separated from CH_3^+ by imposing C_{3v} symmetry. The resulting geometry had an a_1 vibration corresponding to the dissociation, but also an imaginary degenerate (e) vibration for rotation of the H_3 planes. Adjusting the geometry according to the normal mode of this e vibration led via a stepwise procedure to the desired transition structure.

CASSCF Study of Reaction of Singlet Molecular Oxygen with Ethylene. Reaction Paths with C_{2v} and C_s Symmetries

M. Hotokka,*† B. Roos,† and P. Siegbahn‡

Contribution from the Department of Physical Chemistry 2, Chemical Centre, University of Lund, Lund, Sweden, and the Institute of Theoretical Physics, University of Stockholm, Stockholm, Sweden. *Received November 29, 1982*

Abstract: The reaction of singlet molecular oxygen, $O_2(^1\Delta_g)$, with ethylene along four reaction paths of C_{2v} and C_s symmetries has been studied. The present calculations show that formation of the peroxirane intermediate, the first step on the peroxirane pathway to dioxetane, has lower activation energy than that of the biradical pathway. The multiconfiguration CASSCF (complete active space SCF) method and a double-ζ basis (in the final calculations augmented with a single d function on carbon and oxygen) were used. Contracted CI calculations were performed at the key points of the C_s surfaces. Neither of the reaction paths of C_{2v} symmetry were found feasible. In C_s symmetry, the barrier for formation of the peroxirane intermediate is calculated to be 149 kJ/mol. The transition state of C_s symmetry leading to dioxetane via a biradical species is analogous to the C_{2v} one, showing formation of even the second C–O bond at a rather early stage, and has a barrier of 169 kJ/mol. No other low-energy transition states leading to dioxetane via a biradical species have been found in the present CASSCF-CCI calculations.

Since the "rediscovery" of singlet molecular oxygen by Foote and Wexler[1] and Corey and Taylor,[2] the reactions of $O_2(^1\Delta_g)$ with olefins have covered a wide spectrum of practical applications, ranging from polymer chemistry and paper industry to pharmacology.[3-19] The mechanisms of these reactions have been extensively studied, both experimentally and theoretically. However, for an attachment to a double bond, the results seem to be conflicting.[20-38]

The reactions of singlet oxygen with olefins can be classified into three groups: (A) 1,4 addition (endoperoxide formation); (B) 1,3 addition (ene reaction); and (C) 1,2 addition (dioxetane formation). The first one is generally believed to be a concerted [2 + 4] addition which proceeds through a six-membered-ring

†University of Lund, Sweden.
‡University of Stockholm, Sweden.

(1) Foote, C. S.; Wexler, S. *J. Am. Chem. Soc.* **1964**, *86*, 3879.
(2) Corey, E. J.; Taylor, W. C. *J. Am. Chem. Soc.* **1964**, *86*, 3881.
(3) Singlet molecular oxygen: Schaap, A. P., Ed. "Benchmark Papers in Organic Chemistry", Dowden, Hutchinson and Ross, Inc.: Stroudsburg, PA, 1976; Vol. 5.
(4) Singlet oxygen: "Reactions with Organic Compounds and Polymers"; Rånby, B., Rabek, J. F. Eds.; Wiley: New York, 1978.
(5) Singlet oxygen: *Photochem. Photobiol.* **1978**, *28*, No. 4–5.
(6) Singlet oxygen: Wasserman, H. H., Murray, R. W., Eds. "Organic Chemistry"; Academic Press: New York, 1979; Vol. 40.
(7) Kearns, D. R. *Chem. Rev.* **1971**, *71*, 395.
(8) Harrison, J. E.; Watson, B. D.; Schultz, J. *FEBS Lett.* **1978**, *92*, 327.
(9) Keevi, T.; Mason, H. S. *Methods Enzymol.* **1978**, *52*, 3.

0002-7863/83/1505-5263$01.50/0

Scheme I

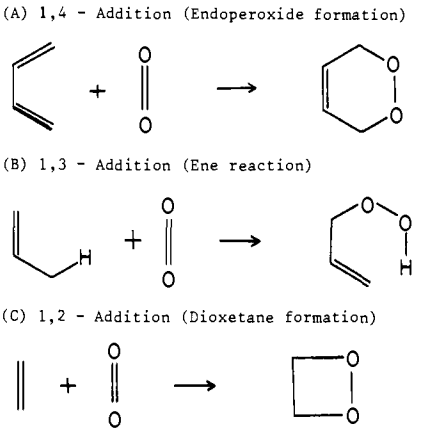

transition state[39,40] although other mechanisms also have been proposed.[41,42] The 1,3 addition has been extensively surveyed recently,[24] the conclusion being that in gas phase this reaction proceeds through a peroxy biradical intermediate or quasi-intermediate. In this paper we study the dioxetane formation reaction (1) by using ethylene as a model olefin.

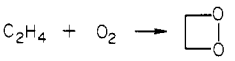

(1)

Several mechanisms have been proposed for dioxetane formation:[23] (C1) the concerted $[{}_{\pi}2_s + {}_{\pi}2_s]$ approach is symmetry forbidden;[43,44] (C2) a stepwise addition via a 1,4 diradical is ruled out because radical inhibitors do not affect the reaction rate;[45] (C3) evidence has been presented for dioxetane formation via 1,4-dipolar species;[23] (C4) the concerted $[{}_{\pi}2_s + {}_{\pi}2_s]$ process becomes allowed when charge transfer from the olefin π orbital to the oxygen π^* orbitals can occur;[7,45] (C5) the cycloaddition might occur via a concerted symmetry-allowed $[{}_{\pi}2_s + {}_{\pi}2_a]$ pathway;[23] (C6) theoretical MINDO calculations support a process where the rate-determining step is formation of a peroxirane.[46-48] Which mechanism is the dominant one has not been unequivocally settled.[23]

Scheme II

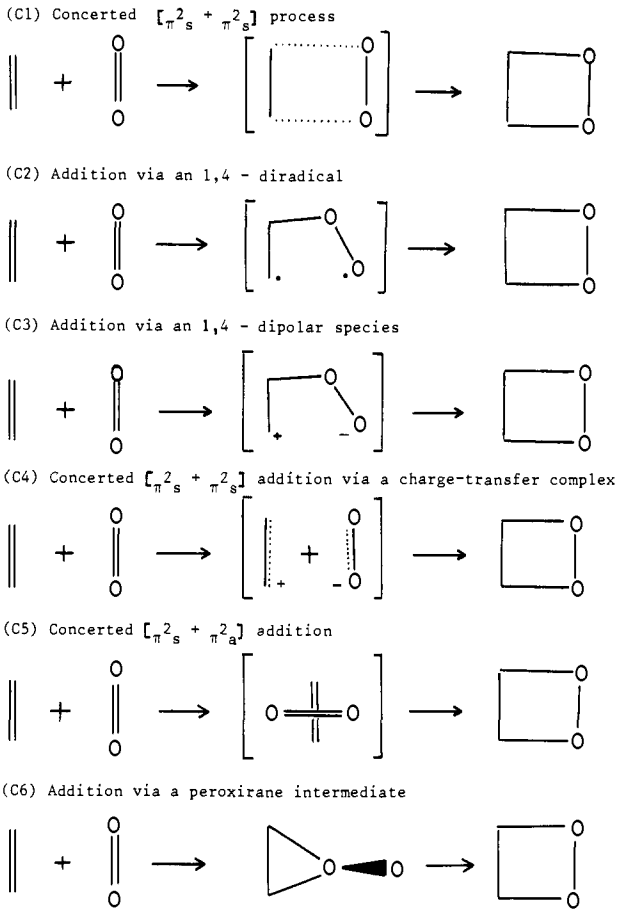

In the present work we explore the four pathways shown in eq 2–5. Orbital and state correlation diagrams would indicate that the concerted path, mechanism 3, is symmetry forbidden.[7,43,44]

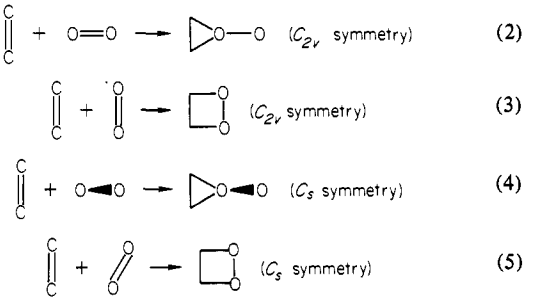

Therefore one would expect to find a rather large barrier and a change of electron configuration during the reaction. Formation

(10) Korycka-Dahl, M. B.; Richardson, T. *CRC Crit. Rev. Food Sci. Nutr.* **1978**, *10*, 209.
(11) Maugh, T. H., II *Science (Washington, D.C.)* **1973**, *182*, 44.
(12) Delmelle, M. *Photochem. Photobiol.* **1979**, *29*, 713.
(13) Elster, E. F. *Encycl. Plant. Physiol., New Ser.* **1979**, *6*, 410.
(14) Chudakov, M. I. *Khim. Drev.* **1980**, 3.
(15) Nimz, H. H.; Turzik, G. *Kemia—Kemi* **1980**, *7*, 477.
(16) MacCallum, J. R. *Dev. Polym. Degradation* **1980**, *1*, 237.
(17) Edwards, J.; Quinn, P. J. *Biochem. Soc. Trans.* **1980**, *8*, 196.
(18) Mach, J.; Veprek-Siska, J. *Chem. Listy* **1980**, *74*, 1.
(19) Gorman, A. A.; Rodgers, M. A. *Chem. Soc. Rev.* **1981**, *10*, 205.
(20) Ashford, R. D.; Ogryzlo, E. A. *J. Am. Chem. Soc.* **1975**, *97*, 3604.
(21) Bartlett, P. D. *Q. Rev., Chem. Soc.* **1970**, *24*, 473.
(22) Bartlett, P. D. *Chem. Soc. Rev.* **1976**, *5*, 149.
(23) Frimer, A. A. *Chem. Rev.* **1979**, *79*, 359.
(24) Harding, L. B.; Goddard, W. A., III *J. Am. Chem. Soc.* **1980**, *102*, 439.
(25) Datta, R. K.; Rao, K. N. *Indian J. Chem., Sect. A* **1979**, *18A*, 102.
(26) Grdina, S. M.; Orfanopoulos, M.; Stephenson, L. M. *J. Am. Chem. Soc.* **1979**, *101*, 3111.
(27) Saito, I.; Matsugo, S.; Matsuura, T. *J. Am. Chem. Soc.* **1979**, *101*, 7332.
(28) Yamaguchi, K.; Fueno, T.; Saito, I.; Matsuura, T. *Tetrahedron Lett.* **1979**, *36*, 3433.
(29) Orfanopoulos, M.; Grdina, S. M.; Stephenson, L. M. *J. Am. Chem. Soc.* **1979**, *101*, 275.
(30) Zaklika, K. A.; Kaskar, B.; Schaap, A. P. *J. Am. Chem. Soc.* **1980**, *102*, 386.
(31) Schaap, A. P.; Zaklika, K. A.; Kaskar, B.; Fung, L. W.-M. *J. Am. Chem. Soc.* **1980**, *102*, 398.
(32) Orfanopoulos, M.; Stephenson, L. M. *J. Am. Chem. Soc.* **1980**, *102*, 1417.
(33) Stephenson, L. M.; Grdina, M. J.; Orfanopoulos, M. *Acc. Chem. Res.* **1980**, *13*, 419.
(34) Paquette, L. A.; Carr, R. V. *J. Am. Chem. Soc.* **1980**, *102*, 7553.
(35) Yamaguchi, K.; Yabushita, S.; Fueno, T. *Chem. Phys. Lett.* **1980**, *70*, 27.
(36) Yamaguchi, K.; Yabushita, S.; Fueno, T. *Chem. Phys. Lett.* **1981**, *78*, 572.
(37) Yamaguchi, K. *Int. J. Quantum Chem.* **1981**, *20*, 393.
(38) Houk, K. N.; Williams, J.C., Jr.; Mitchell, P. A.; Yamaguchi, K. *J. Am. Chem. Soc.* **1981**, *103*, 949.
(39) Gollnick, K.; Haisch, D.; Schade, G. *J. Am. Chem. Soc.* **1972**, *94*, 1747.
(40) Machin, P. J.; Porter, A. E. A.; Sammes, P. G. *J. Chem. Soc., Perkin Trans. 1* **1973**, 404.
(41) Ashford, R. D.; Ogryzlo, E. A. *Can. J. Chem.* **1974**, *52*, 3544.
(42) Dewar, M. J. S.; Thiel, W. *J. Am. Chem. Soc.* **1977**, *99*, 2338.
(43) Kearns, D. R. *J. Am. Chem. Soc.* **1969**, *91*, 6554.
(44) Yamaguchi, K.; Fueno, T.; Fukutome, H. *Chem. Phys. Lett.* **1973**, *22*, 466.
(45) Foote, C. S. *Pure Appl. Chem.* **1971**, *27*, 635.
(46) Dewar, M. J. S.; Griffin, A. C.; Thiel, W.; Turchi, J. *J. Am. Chem. Soc.* **1975**, *97*, 4439.
(47) Dewar, M. J. S.; Thiel, W. *J. Am. Chem. Soc.* **1975**, *97*, 3978.
(48) Dewar, M. J. S. *Chem. Br.* **1975**, *11*, 106.

of peroxirane along path 2 which is the first step in mechanism C6 is claimed to be symmetry allowed.[7] However, Harding and Goddard[24] have pointed out that correlation diagrams are not applicable in this case, and actually one finds a change of electronic structure on path 2. Mechanisms 4 and 5 exhibit no such changes of electron configuration; i.e., they are symmetry allowed.

Method

The Hartree–Fock model gives quite accurate zeroth-order wave functions for stable closed-shell molecules and also in many cases for open-shell systems. However, it breaks down in situations where the electrons undergo substantial rearrangements, as in chemical reactions. There, several electronic configurations are needed even at the zeroth-order level of approximation. An obvious choice, then, is a multiconfiguration (MC) model. In this work the complete active space (CAS) approach[49–51] has been used. The main features of this method are as follows:

The total one-electron space, obtained from the atomic basis by the LCAO procedure, is divided into two parts. Those orbitals used to build the configurations are called primary and the remaining ones secondary orbitals. The primary space comprises inactive orbitals, which are doubly occupied in all configurations, and active orbitals, which describe the changes during the chemical process. The CI wave function is complete in the active subspace. Thus the sometimes difficult choice of important configurations is avoided, and the only remaining "chemical" problem is the choice of the active orbitals. The MC SCF problem is solved with the so-called "super-CI" technique.[51–53]

In the present work the active subspace includes eight orbitals. In terms of the separated molecules C_2H_4 and O_2 they are the ethylene π and π^* orbitals, the bonding and antibonding oxygen σ orbitals, $3\sigma_g$ and $3\sigma_u$, and the oxygen π bond and lone-pair orbitals $1\pi_u$ and $1\pi_g$. These orbitals are needed to describe the formation of the C–O bonds from the O–O and C–C π bonds and restructuring of the oxygen lone pairs. Obviously, this active space is rather limited, in particular as it is lacking the important $2\pi_u$ orbital. The present study, however, includes calculations of four reaction paths for the $O_2 + C_2H_4$ reaction, and a large number of independent calculations (several hundred points on the energy surface) have been performed. With such a prospect in mind it is necessary to limit the size of each calculation as much as possible. Important parts of the energy hypersurface can afterward be studied with higher accuracy.

The preliminary calculations were done by using a double-ζ basis. For carbon and oxygen the (9s5p) primitive set of atom-centered Cartesian Gaussians[54] was contracted to a (4s2p) basis as suggested by Dunning.[55] For hydrogen a (4s) primitive set,[54] contracted to (2s),[55] was used. The exponents for hydrogen were scaled by a factor of 1.24. Finally, the equilibrium geometries of the molecules involved were reoptimized by using the previous double-ζ basis augmented with a single d function on carbon and oxygen. Small nets of points around the transition states on paths 4 and 5 were also computed with the augmented basis set in order to refine the heights of the energy barriers. The exponents $\alpha_d(C) = 0.750$ and $\alpha_d(O) = 0.861$ were obtained through an optimization for the separated molecules at their experimental geometries. Contracted CI (CCI) calculations[59] were performed at the key points on the surfaces with use of the augmented basis set and with the most important CASSCF configurations as reference states.

Calculations

The potential energy surface governing mechanisms 2–5 in the reaction of ethylene with singlet molecular oxygen were studied. The C_{2v} symmetry was assumed to be maintained during the reactions along paths 2 and 3. These two possible mechanisms were studied by using the double-ζ basis only. Two geometrical parameters, the distance between the molecules and the oxygen bond length, were considered as reaction coordinates and varied explicitly while the carbon–carbon bond length and the hydrogen tilt angle were optimized for each point on the surface. The rest of the parameters were kept fixed. The geometrical parameters are summarized in Figure 1a,b. The optimal geometries and the total energies for the reactants, transition states, and products, restricted to C_{2v} symmetry, are given in Table I. The resulting surfaces are visualized in Figure 2. Occupation numbers of the active orbitals are given in Tables III and IV.

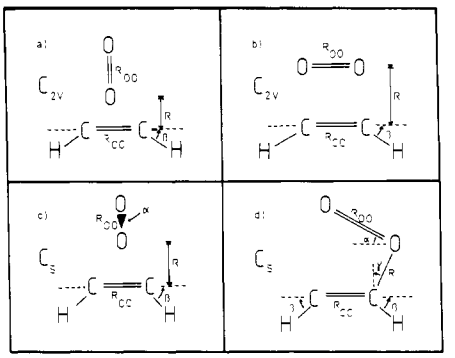

Figure 1. The geometrical parameters for the four reaction paths. The distances R and R_{OO} and the angle α, where relevant, have been treated as reaction coordinates. The distance R_{CC} and the angles β, β', and γ have been optimized at every point.

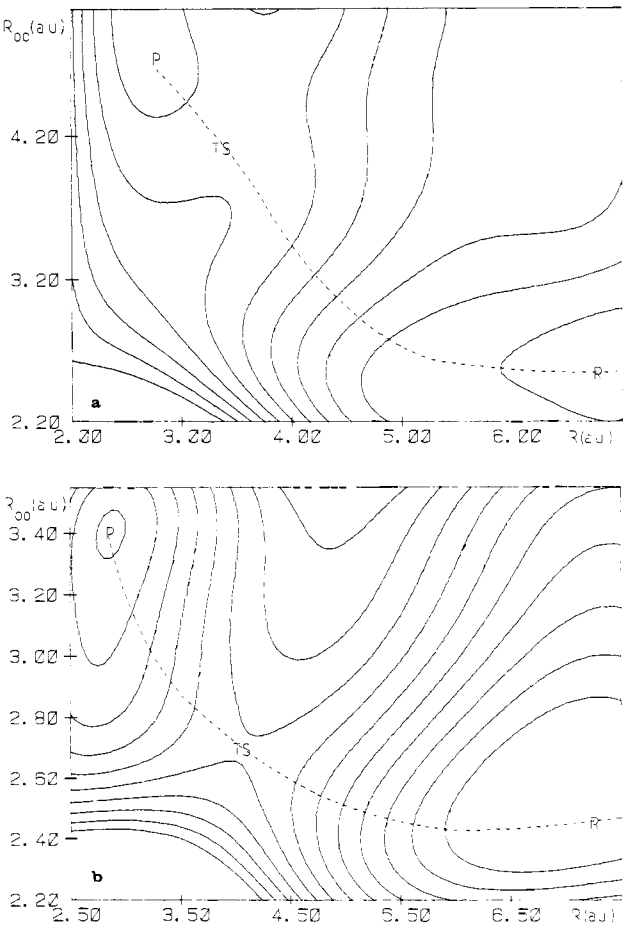

Figure 2. The potential energy surfaces for the C_{2v} reaction mechanisms. The lowest contour line corresponds to −226.7 hartrees, and the interval is 0.02 hartrees. The letters refer to reactants (R), transition states (TS), and products (P). The reaction path on the surface is indicated as a dashed line: (a) path 2; (b) path 3.

The reaction paths of C_s symmetry were surveyed extensively by using the double-ζ basis set. In addition to the reaction coordinates in the C_{2v} cases the oxygen tilt angle was varied explicitly. Again, R_{CC} and the hydrogen tilt angle(s) were optimized at each point. The key features of these surfaces are shown in Table II. Note that the total energies in this table come from calculations with the augmented basis set while those in Table I have been calculated with the double-ζ basis set.

Guided by the results from the calculations with the double-ζ basis set, the critical sections of the potential energy surfaces for

(49) Siegbahn, P.; Heiberg, A.; Roos, B.; Levy, B. *Phys. Scr.* **1980**, *21*, 323.
(50) Roos, B. O.; Taylor, P. R.; Siegbahn, P. E. M.; *Chem. Phys.* **1980**, *48*, 157.
(51) Roos, B. *Int. J. Quantum Chem., Symp.* **1980**, *14*, 175.
(52) Grein, F.; Chang, T. C. *Chem. Phys. Lett.* **1971**, *12*, 44.
(53) Grein, F.; Banerjee, A. *Int. J. Quantum Chem. Symp.* **1975**, *9*, 147.
(54) Huzinaga, S. *J. Chem. Phys.* **1965**, *42*, 1293.
(55) Dunning, T. H., Jr. *J. Chem. Phys.* **1970**, *53*, 2823.

Table I. Optimal Geometries and Total Energies for the Reactants, Transition States, and Products on Paths with C_{2v} Symmetry[a]

	R	R_{OO}	R_{CC}	β	R_{CH}[b]	ΔHCH[b]	E_{tot}
$C_2H_4 + O_2$	∞[c]	132	136	0	107	120	−227.6989
TS (2)	172	201	140	0	107	120	−227.5640
TS (3)	214	148	139	0	107	120	−227.6125
dioxetane	148	164	153	40	107	120	−227.7101
peroxirane	138	256	151	22	107	120	−227.6046

[a] For definitions of the geometrical parameters, see Figure 1. All distances are in pm, bond angles in deg, and energies in Hartrees. The total energies have been obtained with CASSCF method using double-ζ basis sets. [b] A fixed value has been used. [c] 20 au.

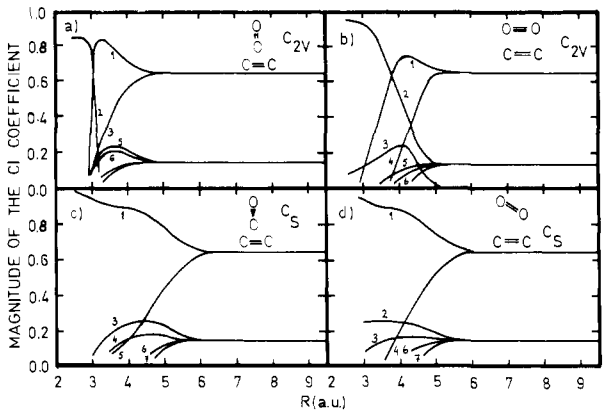

Figure 3. Coefficients of the most important electron configurations along the four reaction paths. The intermolecular distance R indicates how far the reaction has proceeded (cf. Table VII).

reaction paths 4 and 5 were then recomputed by using the augmented basis set. Thus the geometries of the reactants at infinite intermolecular distance were optimized. Also, the geometries of the products, dioxetane and peroxirane molecules, constrained to C_{2v} and C_s symmetries, respectively, were optimized. Near the transition state a mesh of points in the three-dimensional reaction coordinate space was set up. For the transition state leading to peroxirane, the bond length and the hydrogen tilt angle were optimized at each point. As these values agreed with those obtained in the double-ζ calculations, no such optimization was performed on the surface describing mechanism 5. The occupation numbers on the orbitals are summarized in Tables V and VI.

Variations of the CI coefficients along the four reaction paths are depicted in Figure 3. The most important electron configurations of each mechanism are listed in Table VII along with their respective CI coefficients corresponding to the transition state.

Finally, CCI calculations were performed at the key points of the surfaces described in (4) and (5) with the geometries obtained with the CASSCF method at the double-ζ + d level. For each of these two paths, the seven configurations listed in Table VII were used as reference states. The externally truncated CI expansion comprised about 1100 configurations for path 4 and about 1000 configurations for path 5. The uncontracted configuration spaces comprised about 160 000 and 145 000 states, respectively.

Discussion

The energies for reaction paths 2 and 3 are obtained with the double-ζ basis set. All energies for reaction paths 4 and 5 refer to calculations with the augmented basis set and the CASSCF method unless otherwise stated.

1. Reactants. The optimized geometries for the noninteracting reactants are given in Tables I and II. The ethylene molecule is described quite realistically with the present active space and both basis sets. The optimized oxygen bond distance, however, is 10 pm longer than the experimental one, 122.55 pm,[56] at the double-ζ level of approximation. When one d function with α_d = 0.861 (optimized at R_{OO} = 122 pm) is included in the basis set and the original six active orbitals ($3\sigma_g$, $3\sigma_u$, $1\pi_u$, and $1\pi_g$) are used, a much better bond length of 123 pm is obtained. The dissociation energy is improved from 0.058 85 au (1.60 eV) to 0.106 48 au (2.90 eV), as well. Inclusion of an additional π_u orbital, $2\pi_u$, in the active space improves the dissociation energy further to 0.1376 au (3.75 eV). The experimental value for the dissociation energy of $O_2(^1\Delta_g)$ is 4.20 eV.[56] Despite of this slight uncertainty, it is felt that the key features of the present double-ζ plus d-function surfaces mimic the reality and that the conclusions of this work still hold.

2. Products. The equilibrium geometry of peroxirane has lower symmetry than C_{2v}, and therefore path 2 is ruled out. When constrained to C_s symmetry, the peroxirane molecule is found to lie 115 kJ/mol above the reactants or 170 kJ/mol above the dioxetane molecule. At the CCI level of approximation the C–O bond distance seems to increase so that the CCI energy at the CASSCF optimum energy is 133 kJ/mol relative to the reactants and 260 kJ/mol relative to the dioxetane molecule. (There is a large energy lowering due to CI effects in dioxetane.) According to the GVB-CI calculations[24] the energy difference between dioxetane and peroxirane is 220 kJ/mol (or 258 kJ/mol when a correction for zero-point energy is included). The UHF method and 4-31G basis set give a value of 134 kJ/mol.[36] Estimate from a MINDO/3 calculation is 239 kJ/mol.[47] The computed geometry agrees with those obtained in previous works. A comparison is given in Table II.

The outermost oxygen atom has net population of 0.46 electrons in peroxirane while the innermost oxygen atom is almost neutral. The carbon atoms are also slightly negatively charged (−0.19 e). The electrons are donated by the hydrogen atoms which have a positive charge of 0.23 e each. This explains the large dipole moment, 5.69 D. This value is comparable to the results from previous theoretical studies, 5.59 D[24] or 4.26 D.[47]

The optimal geometry of dioxetane is computed within C_{2v} symmetry with the augmented basis set although the molecule is very slightly puckered (the oxygen atoms are shifted about 5 pm from the original plane of the molecule). The present bond lengths and dipole moments agree with those of Harding and Goddard[24] and Yamaguchi et al.[36] However, the energy of the dioxetane molecule relative to separated ethylene and oxygen molecules at the CASSCF level (−53.6 kJ/mol) differs drastically from that obtained by Harding and Goddard (−154.4 kJ/mol) by the GVB-CI method and thermodynamical corrections.[24] This discrepancy is remedied in the CCI calculations where the relative energy of dioxetane was found to be −127.9 kJ/mol.

It may be of some interest to note the great influence of polarization functions on the O–O bond length in dioxetane. The double-ζ CASSCF calculations yield a distance of 164 pm which is reduced to 154 pm by adding one set of 3d functions to the basis set. The corresponding numbers for the oxygen molecule are 132 and 123 pm showing almost the same reduction. The latter value is very close to the experimental bond length in $O_2(^1\Delta_g)$, 122.6 pm,[56] which gives some confidence to the value obtained for dioxetane. The weakness of the O–O bond is noticeable and is illustrated by a large occupation number (0.19 e without and 0.10 e with the 3d functions) of the antibonding orbital σ^*_{OO} (cf. Tables IV and VI).

The charge distribution in dioxetane obtained by Harding and Goddard, as measured by the dipole moment, agrees well with the present calculations. The oxygen atoms have a negative charge of −0.23 e each and the carbons −0.14 e each.

3. Transition States. A natural starting point for studies of reaction mechanisms is to draw orbital and correlation diagrams.[57] The diagrams for the reaction between singlet molecular oxygen and ethylene[7] show that the peroxirane formation (2) should by symmetry allowed while the concerted 1,2 cycloaddition (3) is symmetry forbidden. However, as has been pointed out by

(56) Herzberg, G. "Molecular Spectra and Molecular Structure. I. Spectra of Diatomic Molecules", D. Van Nostrand: New York, 1950.

(57) Woodward, R. B.; Hoffmann, R. "The Conservation of Orbital Symmetry"; Academic Press: New York, 1970.

Table II. Optimal Geometries and the Computed Dipole Moments of the Reactants, Transition States, and Products on Paths with C_s Symmetry[a]

	R	R_{OO}	R_{CC}	α	γ	β	β'	E_{tot} hartree	E_{rel}, kJ/mol	dip. mom
$C_2H_4 + O_2$										
this work	∞[b]	123	135	0	0	0	0	−227.7725	0	
								−227.9020[f]	0[f]	
transition state, path 4										
this work	161	135	141	61.6		11.8		−227.7036	+180.9	4.19
								−227.8452[f]	+149.1[f]	
Dewar[c]	200	122	132						+47.7	
transition state, path 5										
this work	197	127	138	20	5	0	0	−227.6938	+206.6	0.55
								−227.8377[f]	+168.7[f]	
peroxirane										
this work	129	152	146	67.9		11.8		−227.7288	+114.7	5.69
								−227.8513[f]	+133.2[f]	
Harding and Goddard[d]	124	154	150	60.5					+69.0	5.59
Yamaguchi et al.[e]	128	165	146	64.6						
dioxetane										
this work	148	153	152	0		36.4	36.4	−227.7929	−53.6	3.67
								−227.9507[f]	−127.8[f]	
Harding and Goddard[d]	146	153	157	0					−154.4	3.63
Yamaguchi et al.[e]	147	149	152	0						

[a] A comparison to some previous theoretical work is given, as well. For definitions of the geometrical parameters, see Figure 1c,d. All distances are in pm, bond angles in deg, and dipole moments in debyes. All energies refer to double-ζ plus d function calculations. [b] 20 au. [c] Reference 47. [d] Reference 24. [e] Reference 36. [f] CCI result.

Table III. Occupation Numbers of the Active Orbitals at the Key Points on the Surface for Reaction Mechanism 2[a]

	$R = \infty$	transitn state	peroxirane
$8a_1$	(σ_{OO}) 1.9341	1.9027	(σ_{OO}) 1.9559
$10a_1$	(σ^*_{OO}) 0.0675	0.0969	(σ^*_{OO}) 0.0444
$9a_1$	(π_{CC}) 1.9072	0.6033	(π_{CC}) 0.5853[b]
$3b_1$	(π_{OO}) 1.9116	1.9079	(σ_{CO}) 1.9521
$4b_1$	(π^*_{OO}) 1.0814	1.7207	(η_O) 1.7301[c]
$5b_1$	(π^*_{CC}) 0.0928	0.0948	(σ^*_{CO}) 0.0488
$2b_2$	(π_{OO}) 1.9129	1.9979	(π_{OO}) 1.9988
$3b_2$	(π^*_{OO}) 1.0925	1.6758	(π^*_{OO}) 1.6845

[a] The inactive orbitals are all doubly occupied and therefore omitted. The character of the orbitals is indicated in parentheses. The numbers refer to CASSCF calculations with the double-ζ basis. [b] This orbital has to a large extent retained its ethylene π character. [c] This orbital is predominantly of 2p character residing at the outermost oxygen atom.

Table IV. Occupation Numbers of the Active Orbitals at the Key Points on the Surface for Reaction Mechanism 3[a]

	$R = \infty$	transitn state	dioxetane
$6a_1$	(σ_{OO}) 1.9198	1.8850	(σ_{OO}) 1.8151
$7b_1$	(σ^*_{OO}) 0.0820	0.1179	(σ^*_{OO}) 0.1891
$7a_1$	(π_{CC}) 1.9073	1.8666	(σ_{CO}) 1.9688
$8a_1$	(π_{OO}) 1.8941	1.2508	(σ^*_{CO}) 0.0407
$5b_1$	(π^*_{OO}) 1.0814	0.8204	(σ_{CO}) 1.9599
$6b_1$	(π^*_{CC}) 0.0928	0.1396	(σ^*_{CO}) 0.0311
$2b_2$	(π_{OO}) 1.8997	1.9910	(π_{OO}) 1.9993
$2a_2$	(π^*_{OO}) 1.1230	1.9287	(π^*_{OO}) 1.9958

[a] The inactive orbitals are all doubly occupied and therefore omitted. The character of the orbitals is indicated in parentheses. The numbers refer to CASSCF calculations with the double-ζ basis.

Harding and Goddard,[24] the relevant state of the oxygen molecule, $^1\Delta_{gs}$, has 1,2-biradical character. Implicit in the correlation diagrams is the assumption of the reactant electronic structure involving only doubly occupied orbitals (either π_{gx}^2 or π_{gy}^2), thus invalidating the analyses. Similarly, the orbital phase continuity analysis[58] of Yamaguchi et al.[44] does not apply here.[24]

Table V. Occupation Numbers of the Active Orbitals at the Key Points on the Surface for Reaction Mechanism 4, Calculated with the Augmented Basis Set[a]

	$R = \infty$	transitn state	peroxirane
9a′	(σ_{OO}) 1.9413	1.9644	(σ_{OO}) 1.9972
13a′	(σ^*_{OO}) 0.0604	0.0455	(σ^*_{OO}) 0.0358
11a′	(π_{CC}) 1.8982	1.9092	(σ_{CO}) 1.9653
12a′	(π^*_{OO}) 1.0986	0.1185	(σ^*_{CO}) 0.0517
4a″	(π_{OO}) 1.9139	1.9876	(σ_{CO}) 1.9985
6a″	(π^*_{CC}) 0.1018	0.0908	(σ^*_{CO}) 0.0391
10a′	(π_{OO}) 1.9163	1.9562	(π_{OO}) 1.9514
5a″	(π^*_{OO}) 1.0695	1.9278	(π^*_{OO}) 1.9611

[a] The inactive orbitals are all doubly occupied and are therefore omitted. The character of the orbitals is indicated in parentheses.

Table VI. Occupation Numbers of the Active Orbitals at the Key Points on the Surface for Reaction Mechanism 5, Calculated with the Augmented Basis Set[a]

	$R = \infty$	transitn state	dioxetane
10a′	(σ_{OO}) 1.9198	1.9525	(σ_{OO}) 1.9042
15a′	(σ^*_{OO}) 0.0820	0.0491	(σ^*_{OO}) 0.0988
11a′	(π_{CC}) 1.9073	1.9332	(σ_{CO}) 1.9709
12a′	(π_{OO}) 1.8941	1.8629	(σ_{CO}) 1.9612
13a′	(π^*_{OO}) 1.0814	1.0927	(σ^*_{CO}) 0.0386
14a′	(π^*_{CC}) 0.0928	0.1030	(σ^*_{CO}) 0.0302
3a″	(π_{OO}) 1.8997	1.9290	(π_{OO}) 1.9992
4a″	(π^*_{OO}) 1.1230	1.0785	(π^*_{OO}) 1.9969

[a] The inactive orbitals are all double occupied and are therefore omitted. The character of the orbital is indicated in parentheses.

The transition state on the peroxirane pathway (2) lies at R = 170 pm R_{OO} = 200 pm. The shape of the potential surface in Figure 2 shows that the exact position of the transition state is difficult to determine. The energetics of this reaction path is partly explained by the fact that neither of the dominant electron configurations for the reactants becomes the dominant electron configuration of the product during the reaction; i.e., the reaction is symmetry forbidden. Also, the surface is of limited interest because the product, peroxirane, has lower symmetry than C_{2v}. Constrained to C_{2v} symmetry, the peroxirane molecule is calculated to lie 246 kJ/mol above the reactants and the barrier on the pathway leading to this product is 350 kJ/mol. The height of the barrier is roughly halved when going to C_s symmetry. The value obtained with the double-ζ basis set is 166 kJ/mol.

(58) Goddard, W. A., III *J. Am. Chem. Soc.* **1972**, *94*, 793.
(59) Siegbahn, P. E. M. *Chem. Phys.* **1982**, *66*, 443.
(60) Yamaguchi, K.; Yabushita, S.; Fueno, T.; Houk, K. N. *J. Am. Chem. Soc.* **1981**, *103*, 5043.

Table VII. The Most Important Electron Configurations of the Four Reactions and Their CI Coefficients at the Respective Transition States[a]

path 2	occupation numbers of the orbitals $8a_1$	$9a_1$	$10a_1$	$3b_1$	$4b_1$	$5b_1$	$2b_2$	$3b_2$	CI coeff
1	2	0	0	2	2	0	2	2	0.80
2	2	2	0	2	2	0	2	0	−0.48
3	2	2	0	2	0	0	2	2	−0.16
4	1	0	1	1	2	1	2	2	−0.13
5	0	0	2	2	2	0	2	2	−0.12
6	2	0	0	0	2	2	2	2	−0.12

path 3	occupation numbers of the orbitals $6a_1$	$7a_1$	$8a_1$	$5b_1$	$6b_1$	$7b_1$	$2b_2$	$2a_2$	CI coeff
1	2	2	2	0	0	0	2	2	0.71
2	2	2	0	2	0	0	2	2	−0.55
3	2	1	1	1	1	0	2	2	−0.24
4	2	2	2	2	0	0	2	0	−0.16
5	0	2	2	0	0	2	2	2	−0.14
6	0	2	0	2	0	2	2	2	−0.13
7	1	2	1	1	0	1	2	2	−0.11

path 4	occupation numbers of the orbitals 9a'	10a'	11a'	12a'	13a'	4a''	5a''	6a''	CI coeff
1	2	2	2	0	0	2	2	0	0.94
2	2	2	1	1	0	2	1	1	−0.15
3	2	2	0	2	0	2	2	0	−0.13
4	2	0	2	0	0	2	2	2	−0.11
5	2	2	2	2	0	2	0	0	<0.10
6	1	2	1	1	1	2	2	0	<0.10
7	0	2	2	0	2	2	2	0	<0.10

path 5	occupation numbers of the orbitals 10a'	11a'	12a'	13a'	14a'	15a'	3a''	4a''	CI coeff
1	2	2	2	0	0	0	2	2	0.88
2	2	2	0	2	0	0	2	2	−0.26
3	2	0	2	0	2	0	2	2	−0.14
4	2	2	2	2	0	0	2	0	−0.12
5	2	1	1	1	1	0	2	2	0.12
6	2	2	2	2	0	0	0	2	<0.10
7	2	0	2	2	2	0	2	0	<0.10

[a] The inactive orbitals are double occupied in all configurations and are therefore omitted.

Analogously, symmetry forbids reaction path 3 which describes a concerted 1,2 cycloaddition with transition state at R = 214 pm, R_{OO} = 148 pm, and 225 kJ/mol above the reactants. The evolution of the coefficients of the most important configurations during the process is depicted in Figure 3b. The hump observed at the transition state describes the most important open-shell configuration. Its existence explains why the first attempts with a closed-shell MC method were ruined (cf. Table VII).

In the reduced symmetry the peroxirane pathway (4) has a transition state at R = 161 pm and R_{OO} = 135 pm which lies 181 kJ/mol above the reactants and 66 kJ/mol above the product. It is seen in Figure 3c that this mechanism is symmetry allowed. As can be expected on basis of Hammond's postulate, the transition state resembles the product. This resemblance is reflected in the elongated C–C and O–O bonds as well as in the electronic structure of the system. The 12a' and 5a'' orbitals are already quite strongly deformed at the transition state to produce the new bonds between oxygen and carbon. Even the dipole moment of the transition state, 4.19 D, indicates that the electronic structure is rather similar to that in peroxirane. The Mulliken population analysis shows that the outermost oxygen atom has gained 0.36 e while the innermost oxygen atom is virtually neutral. The carbons have an excess of 0.25 e each.

Mechanism 5 leading to dioxetane via a biradical intermediate is found to be about 25 kJ/mol less favorable than the peroxirane formation step in mechanism 4. This situation is not essentially altered in the CCI calculations. On this path the first oxygen–carbon bond starts to form at the intermolecular distance R = 200–210 pm. This is reflected in the deformation of the 11a' orbital to extend over both molecules. Shortly afterward the oxygen molecule starts to bend to become parallel with the ethylene molecule. Thus, according to the CASSCF calculations, the system tends to form the four-ring structure of dioxetane at a rather early stage. This bending motion is the most difficult part of the reaction because here the supermolecule approaches the symmetry-forbidden C_{2v} path (although the C_s path remains symmetry allowed as is seen in Figure 3d). If the oxygen molecule is brought to the same distance R from the ethylene molecule as found at the transition state but without forcing it to bend, the total energy of the system is much lower, 128 kJ/mol above the separate molecules or almost 80 kJ/mol below the transition state. However, no low-energy path leading to dioxetane via a strongly bound biradical species is found when the oxygen is pushed nearer the ethylene molecule along this valley.

Conclusions

Four possible mechanisms for the reaction of ethylene and singlet molecular oxygen, $O_2(^1\Delta_g)$, have been studied by using a double-ζ and double-ζ plus d function basis set. The present CASSCF-CCI calculations constitute for the present the most thorough mapping of the potential surfaces describing the reaction mechanisms 2–5. They show that formation of the peroxirane intermediate, the first step on the peroxirane pathway to dioxetane, has lower activation energy than the biradical pathway. Those paths that belong to C_{2v} symmetry are found to be unfeasible. Path 2 exhibits an energy barrier of 350 kJ/mol and path 3 one of 225 kJ/mol. The explanations for these high barriers are straightforward: Mechanism 2 suffers from a serious symmetry restriction as the product peroxirane, has lower symmetry than C_{2v}. Mechanism 3 is found to be symmetry forbidden as is seen in Figure 3b. Reaction mechanisms 4 and 5 are both symmetry allowed but they, too, have rather high barriers of 181 and 207 kJ/mol, respectively, in the CASSCF approximation. The barriers obtained with the CCI method are 149 and 169 kJ/mol, respectively. The biradical path (5) to dioxetane is about 20 kJ/mol less favorable than path 4 leading to peroxirane. Substitution of the hydrogens at both ends of the C-C bond probably affects strongly this difference and may even switch the order of the reaction paths. This seems to be in accordance with the experimental findings, as well.[29] No low-energy pathway leading to a strongly bound biradical species of type 5 with a short (~150 pm) CO bond length has been found in the present work.

Unfortunately it is presently economically impossible to survey the totally unsymmetrical pathways. A particularly interesting candidate for closer study would of course have been the step from peroxirane to dioxetane. As there is no conclusive experimental evidence for a peroxirane intermediate, one must conclude that the conversion of peroxirane to dioxetane occurs much faster than the initial reaction (4)—or that there is an altogether different and more favorable pathway from ethylene and singlet oxygen to dioxetane.

Dewar and Thiel report MINDO/3 calculations[47] that suggest a barrier of 142 kJ/mol for the step from peroxirane to dioxetane which would make this step rate determining. When this barrier height is added on top of the present CASSCF energy for peroxirane, the transition state is found 257 kJ/mol above the reactants. This activation energy seems rather high, however. It should not be energetically very unfavorable to distort the peroxirane to allow the conversion to dioxetane to occur. The cost for breaking one of the CO bonds can be estimated to be roughly 100 kJ/mol from the study of barriers to interconversion of 2-hydroxyethyl cations via oxiranium ion.[61] This energy requirement is counterbalanced by the energy gain obtained when simultaneously forming the new CO bond to give dioxetane. Therefore the barrier is expected to be well below 100 kJ/mol.

A reaction mechanism where the oxygen molecule attacks one end of the ethylene molecule with the outermost oxygen atom

(61) Hopkinson, A. C.; Lien, M. H.; Csizmadia, I. G.; Yates, K. *Theor. Chim. Acta* **1978**, *47*, 97.

pointing away from the double bond (i.e., with $\alpha > 180°$, cf. Figure 1) as advocated by Yamaguchi et al.[60] is an interesting proposition. Subsequently a rotation around the newly formed CO bond gives dioxetane in a process which involves a totally asymmetrical transition state.

The conclusion of this paper is, then, that the dioxetane pathway has somewhat higher barrier than the peroxirane pathway, provided that the conversion of peroxirane to dioxetane is not the rate-determining step. The present study is noncommital to the totally unsymmetrical reaction paths.

Acknowledgment. Many encouraging discussions with Professor P. Pyykkö are gratefully acknowledged. M. H. wishes to thank The Academy of Finland for financial support. Besides the Finnish Universities' UNIVAC 1108, computer resources have been made available to us by the Computing Centre at University of Oulu and the Computer Centre in Lund.

Registry No. Oxygen, 7782-44-7; ethylene, 74-85-1.

Clustering of Hydrophobic Ions in the Presence and Absence of the Polysoap Poly(vinylbenzo-18-crown-6)

Bruno Roland and Johannes Smid*

Contribution from the Chemistry Department, College of Environmental Science and Forestry, State University of New York, Syracuse, New York 13210. *Received January 19, 1983*

Abstract: Measurements of optical absorption and fluorescence spectra and of turbidity in dilute aqueous solutions of 4-((1-pyrenyl)butyl)trimethylammonium bromide (PN^+) and sodium tetraphenylborate (BPh_4^-) point to the formation of stable aggregates with the preferred stoichiometry $(PN^+)_2(BPh_4^-)_3$. The complex only shows the pyrene excimer emission, which disappears, together with the coacervate phase, on adding an excess of the polysoap poly(vinylbenzo-18-crown-6) (P18C6). The presence of BPh_4^- ions greatly enhances the binding of PN^+ to P18C6, as the binding capacity of the polymer is increased from one PN^+ molecule per 26 monomer base units in the absence of BPh_4^- to about one PN^+ per 2.5 monomer units in the presence of BPh_4^-. It is speculated that under these saturation conditions the pyrene moieties of the $(PN^+)_2(BPh_4^-)_3$ complex are inserted in between adjacent benzocrown ether ligands with the $-N^+(CH_3)_3$ groups protruding into the aqueous phase and paired to BPh_4^- ions.

Formation of 1:1 ion-pair complexes in dilute aqueous solutions of hydrophobic solutes of opposite charge and the subsequent appearance of a complex coacervate phase have been well documented.[1,2] In a recent communication, Atik and Singer[3] reported the formation of premicellar aggregates between the fluorophor sodium 5-(1-pyrenyl)pentanoate (PP^-) and cationic surfactants (S^+) such as cetyltrimethylammonium chloride (CTAC). They deduced from ESR studies with a surfactant nitroxyl radical that the predominant aggregate structure was $(PP^-)_2(S^+)_3$. The latter complex, with two pyrene moieties in close proximity, exhibited exclusively the characteristic pyrene excimer emission. An earlier report by Davis[4] on the fluorescence of potassium 4-(1-pyrenyl)butanoate (PB^-) in the presence of cetyltrimethylammonium bromide (CTAB) showed complete conversion of monomer into excimer emission when the ratio CTAB/PB^- reached the value 1.5 for $[PB^-] = 8.8 \times 10^{-5}$ M, although no conclusion was drawn as to the possible significance of this observation in terms of a specific aggregate stoichiometry.

In recent years we studied in detail the polysoap-type properties of poly(vinylbenzo-18-crown-6) (P18C6), a polymer which binds a variety of neutral and ionic organic solutes.[5-9] While investigating the interaction of P18C6 with cationic and anionic pyrene derivatives[10] we observed that the binding of 4-((1-pyrenyl)butyl)trimethylammonium bromide (PN^+) to P18C6 in water can

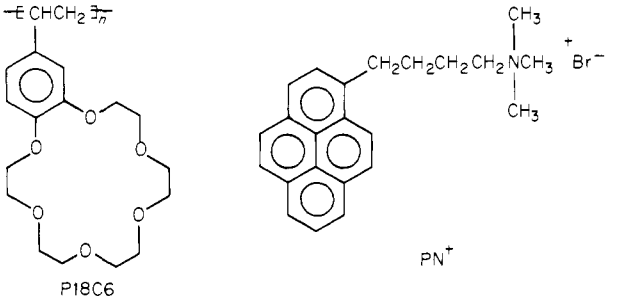

be dramatically enhanced by adding minute amounts of sodium tetraphenylborate. Subsequent studies on dilute solutions of PN^+ and BPh_4^- in the presence and absence of P18C6 indicate the presence of complexes of the type $(PN^+)_2(BPh_4^-)_3$, similar to the premicellar aggregates found by Atik and Singer for the anionic pyrene derivative and the cationic surfactant molecule. Apparently, such complexes between hydrophobic ions may be more common, and their formation profoundly affects their binding to polysoap-type macromolecules like P18C6.

Experimental Section

Materials. 4-((1-Pyrenyl)butyl)trimethylammonium bromide was obtained for Molecular Probes, Inc., while sodium tetraphenylborate of 99.5% purity was a Fisher product. The synthesis of poly(vinylbenzo-18-crown-6) was reported earlier.[11] The number average molecular weight of the polymer as measured by osmometry was 110000 (DP_n = 320).

Measurements. Optical spectra were recorded on a Beckman Acta M VI spectrophotometer, and fluorescence spectra were obtained by means of a Perkin-Elmer 650-10S spectrofluorimeter. Turbidities of aqueous mixtures of PN^+Br^- and $NaBPh_4$ were measured with a DRT-100 tur-

(1) Mukhayer, G. I.; Davis, S. S. *J. Colloid Interface Sci.* **1975**, *53*, 224.
(2) Tomlinson, E.; Davis, S. S. *J. Colloid Interface Sci.* **1980**, *74*, 349.
(3) Atik, S. S.; Singer, L. A. *J. Am. Chem. Soc.* **1979**, *101*, 6759.
(4) Davis, G. A. *J. Chem. Soc., Chem. Commun.* **1973**, 728.
(5) Wong, L.; Smid, J. *J. Am. Chem. Soc.* **1977**, *99*, 5637.
(6) Shah, S. C.; Smid, J. *J. Am. Chem. Soc.* **1978**, *100*, 1426.
(7) Kimura, K., Smid, J. *Macromolecules* **1982**, *15*, 966.
(8) Smid, J. *Pure Appl. Chem.* **1982**, *54*, 2129.
(9) Wong, K. H.; Kimura, K.; Smid, J. *J. Polym. Sci., Polym. Chem. Ed.* **1983**, *21*, 579.
(10) Roland, B.; Smid, J.; to be published.
(11) Kopolow, S.; Hogen Esch, T. E.; Smid, J. *Macromolecules* **1973**, *6*, 133.

0002-7863/83/1505-5269$01.50/0